

## Generation of Atomic Iodine in RF Discharge for DOIL (Discharge Oxygen Iodine Laser)\*

I. Picková<sup>1,2</sup>, J. Schmiedberger<sup>1</sup>, V. Jirásek<sup>1</sup>, M. Čenský<sup>1</sup>

<sup>1</sup>Institute of Physics, Academy of Sciences of the CR, v.v.i., Division of High-Power Systems, Department of Chemical Lasers, Na Slovance 2, 182 21 Praha 8, Czech Republic

<sup>2</sup>Charles University in Prague, Faculty of Mathematics and Physics, Department of Surface and Plasma Science, V Holešovičkách 2, 180 00 Praha 8, Czech Republic

**Abstract:** In this article we describe our new experimental device for generation of atomic iodine in a RF discharge and the first results obtained with this device. The atomic iodine generator is the first part of proposed DOIL (discharge oxygen-iodine laser) system. In this laser, atomic iodine is the lasing medium, while excited oxygen molecule is the source of energy for iodine excitation. Iodine donor (molecule containing iodine – CH<sub>3</sub>I, CF<sub>3</sub>I) is dissociated in the discharge and then injected into the supersonic flow of primary gas. This gas is nitrogen in the present experiments, it will later contain excited oxygen and a buffer gas.

**Keywords:** discharge oxygen-iodine laser, atomic iodine, RF discharge.

### 1. Introduction

COIL (chemical oxygen-iodine laser) and DOIL (discharge oxygen-iodine laser) are the lasers, which radiate on the magnetic dipole transition  $I(^2P_{1/2}) - I(^2P_{3/2})$  of atomic iodine (wavelength 1315 nm – near infrared region). These lasers obtain energy for iodine excitation in collisions with excited oxygen molecule (so called singlet oxygen  $O_2(^1g)$  – first electronically excited state of  $O_2$ , metastable state with extremely long radiative lifetime ~ tens of minutes).

For successful COIL (and also DOIL) laser operation we need to accomplish the following tasks: generation of iodine atoms, generation of singlet oxygen and finally, mixing these two, the gas flows together so iodine atoms can be excited in collisions.

In a classical COIL atomic iodine is generated from  $I_2$ , which is dissociated in collisions with singlet oxygen (usually 4–6 oxygen molecules are consumed for dissociation of one  $I_2$  molecule). Singlet oxygen is produced in the chemical reaction of liquid mixture of  $H_2O_2$  and KOH with  $Cl_2$  gas. To improve laser operation, different ways of atomic iodine generation were examined, so the singlet oxygen energy can be saved for iodine excitation [1–3].

In DOIL the singlet oxygen is generated in a discharge. Atomic iodine can be generated also in discharge. Various experiments were also performed with iodine generation in discharge for COIL, to improve its operation. Various types of discharge (DC, microwave, RF) and various iodine donors ( $CH_3I$ ,  $CF_3I$ , HI,  $I_2$ ) have been examined in different research groups [4–6].

*\*) Dedicated to Professor Peter Lukáč on the occasion of his 70th birthday.*

In our group, we are currently constructing a new DOIL system. Its first part – the atomic iodine RF discharge generator, has already been built and first experiments have been performed. Various iodine donors are considered:  $\text{CH}_3\text{I}$ ,  $\text{CF}_3\text{I}$  (both already used but experiments with them would continue),  $\text{HI}$ ,  $\text{I}_2$ ,  $\text{C}_3\text{F}_7\text{I}$ . Flows from iodine and singlet oxygen generators will be mixed and, at the end, we expect to successfully operate DOIL, whose full radiation power should be some tens of watts.

Further, the most suitable iodine donor will be selected. Criterion will be not only good physical and chemical properties and operability, but also economical point of view will be taken into account.

## 2. Experimental setup

The main part of the new experimental device is the injector body, which also serves as a discharge chamber and forms a supersonic double slit nozzle, see Fig. 1, part 4, Fig. 2 and [7]. Primary gas (which is now  $\text{N}_2$  and later it will be mixture  $\text{He} + \text{O}_2^*$ ) flows around the injector while secondary gases ( $\text{Ar} + \text{He} + \text{iodine donor}$ ) are introduced into the discharge chamber, where an electrode-coupled RF discharge is operated and atomic iodine is generated by dissociation of an iodine donor. Discharge products are injected through two rows of circular orifices (diameter 2.2 mm) to the primary gas flow into the supersonic nozzle. Shape of this body and its dimensions were designed by means of the 2-D method of characteristics, 1-D isentropic flow calculations and CFD (computational fluid dynamics) modelling.

The discharge is operated in the cylindrical duct (the middle hole in Fig. 2) inside the discharge chamber/injector. The duct is 70 mm long and has 9 mm in diameter and its walls are grounded. An axially inserted tungsten electrode is powered by RF voltage. In the injector body there are also two channels for water or ethanol cooling/heating.

Different conditions for RF discharge operation will be examined (different frequencies, cw or periodically pulsed mode, different flow rates and pressures, subsonic and supersonic flow). Our RF power source can deliver frequencies from 20 to 100 MHz in cw and pulsed mode and RF power up to 500 W.

The selection of materials used for construction of the discharge atomic iodine generator device is also important. The injector body is made of pure aluminum, which has good electric and thermal conductivity, while the supersonic cavity is made of Plexiglas (transparent plastic material) covered with glass panes on inner walls. These materials are resistant to corrosion caused by  $\text{I}_2$  and are not efficient quenchers of singlet oxygen.

## 3. Diagnostic techniques

Our main diagnostic tool for the first experiments was absorption spectroscopy on the wavelength 1 315 nm, which is the wavelength of a transition between ground and excited level of atomic iodine ( $\text{I}(^2\text{P}_{3/2}) \rightarrow \text{I}(^2\text{P}_{1/2})$ ). We measured the vertical profiles of atomic iodine absorption in the afterglow in different distances from output nozzles of discharge chamber. These measurements were naturally accompanied by measurements of gas flow rates and pressures (the most important were the data from discharge chamber and from cavity with afterglow).

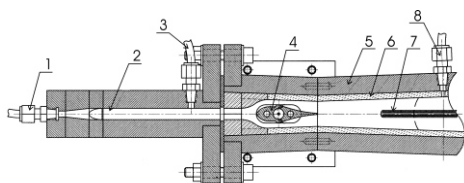


**Fig. 1.** A side view of discharge atomic iodine generator device: 1 – inlet of primary gas flow; 2 – subsonic duct; 3 – pressure detection in subsonic duct; 4 – discharge chamber, iodine injector/double slit supersonic nozzle; 5 – Plexiglas supersonic cavity; 6 – thin pane (glass); 7 – Pitot tube; 8 – pressure detection in supersonic cavity.

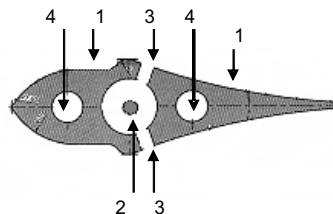


**Fig. 2.** Detail view of the discharge chamber, 1 – discharge chamber body working as outer (grounded) electrode, 2 – inner electrode inserted axially in the discharge chamber, 3 – output orifices, 4 – channel for ethanol/water cooling / heating.

We were able to determine atomic iodine concentration, dissociation fraction and also the temperature in the afterglow from measured data.

In ongoing experiments, we intend to use also emission spectroscopy diagnostics for wavelengths between 600 and 1 700 nm. The emission spectroscopy data will indicate the presence of other species in plasma and will help us to understand more of the processes taking place in the discharge. Up to now the literature search has yielded only information about basic theories [8] and some already measured and tabulated data [9].

#### 4. Experimental results

In first measurements we examined two iodine donors –  $\text{CH}_3\text{I}$  and  $\text{CF}_3\text{I}$ . These donors were injected into the discharge chamber together with secondary (buffer) gases (Ar + He). Power applied on the discharge was varied from 45 to 250 W and the frequency was kept at 40 MHz. The pressure in the discharge chamber was between 2.0 and 3.2 kPa (depending upon the gas flows of buffer gases and iodine donor), pressure in the cavity (afterglow) was between 140 and 850 Pa (lower pressure was when throttling valve at the output to the vacuum pump was opened, which, with sufficient gas flows, enabled supersonic flow in the afterglow cavity). For  $\text{CF}_3\text{I}$  the experiments were performed at subsonic speed, while for  $\text{CH}_3\text{I}$  both conditions for subsonic and supersonic speed in the afterglow were examined. In fact, most experiments were performed under subsonic conditions, the main reason being that at supersonic flow speeds the pressure in the cavity was low and the absorption spectroscopy signal was rather noisy.

For both iodine donors vertical profiles of atomic iodine number density in the afterglow were measured, the results for  $\text{CH}_3\text{I}$  are shown in Fig. 3. These profiles are flat and homogeneous for a low RF power, but later experiments showed that for higher  $\text{N}_2$  flows the profiles became sharper with maximum in the middle of the cavity height and also homogeneity was lower.

The dissociation fraction ( $\alpha_{\text{diss}}$ ) of  $\text{CH}_3\text{I}$  and  $\text{CF}_3\text{I}$  can be calculated from the measured concentration of atomic iodine in the cavity, temperature and flow rates of gases. The

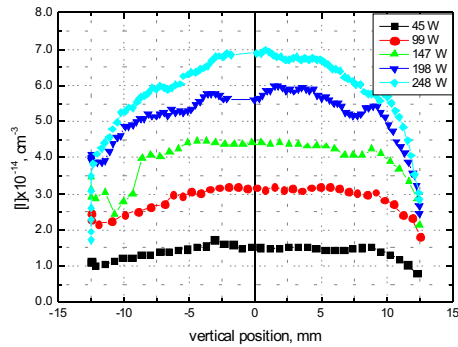


**Fig. 3.** Vertical profile of atomic iodine number density at five values of absorbed RF power.  $p_{\text{cav}} = 780$  Pa; flow rates (mmol/s): 0.73  $\text{CH}_3\text{I}$ ; 1.96 Ar; 1.92 He; 20.6  $\text{N}_2$ , subsonic flow, position 188.2 mm downstream of the injection point.

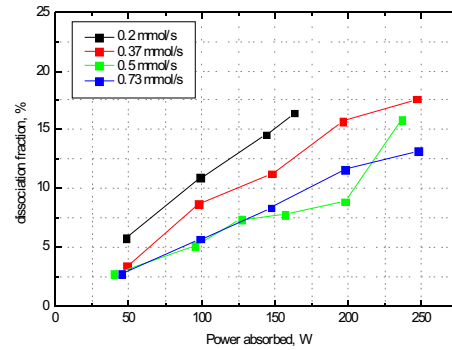


**Fig. 4.** Dependence of  $\text{CH}_3\text{I}$  dissociation fraction on the absorbed RF power for different  $\text{CH}_3\text{I}$  flow rates,  $p_{\text{cav}} = 560\text{--}780$  Pa; flow rates (mmol/s): 1.9 Ar; 1.9 He; 10–20  $\text{N}_2$ .

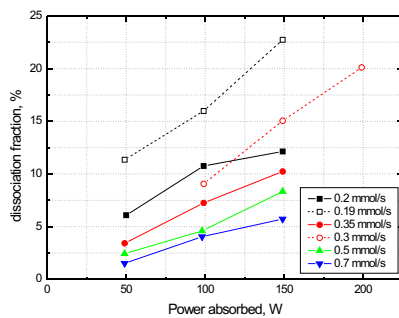


**Fig. 5.** Dependence of  $\text{CF}_3\text{I}$  dissociation fraction on absorbed RF power for different  $\text{CF}_3\text{I}$  flow rates,  $p_{\text{cav}} = 500$  Pa; flow rates (mmol/s): 1.9 Ar (solid lines) or 3.1 (dashed lines); 1.9 He (solid) or 0 He (dashed); 10–20  $\text{N}_2$ .

increasing RF power and with increasing donor flow rate. The highest iodine number density was about  $7 \cdot 10^{14} \text{ cm}^{-3}$ .

First results for  $\text{CF}_3\text{I}$  were obtained only for the subsonic flow. The flow rate of this donor was between 0.18 and 0.91 mmol/s. Pressures in the discharge chamber were between 2.2 and 4.6 kPa, pressures in the cavity were between 520 and 680 Pa.

We can observe in Fig. 5 the dissociation fraction of  $\text{CF}_3\text{I}$  as a function of the absorbed RF power with  $\text{CF}_3\text{I}$  flow rates as a parameter. It is obvious that, with increase of the donor flow rate,  $d_{\text{diss}}$  is decreasing, because the energy per a single donor molecule is decreasing, too. Another interesting effect – substantial increase in  $d_{\text{diss}}$  – arises from the elimination of He from secondary gas flow (dashed lines in Fig. 5). The highest value of the iodine

highest measured  $d_{\text{diss}}$  was about 17% for  $\text{CH}_3\text{I}$  (see Fig. 4) and about 22.5% for  $\text{CF}_3\text{I}$  at the flow rate 0.19 mmol/s with buffer gas being Ar only (see Fig. 5). These curves also show no significant saturation. We can expect, that by increasing the RF power or by changing other experimental conditions, we would be able to reach even higher values of dissociation fraction  $d_{\text{diss}}$ .

In Fig. 4 there are shown dependencies of  $\text{CH}_3\text{I}$  dissociation fraction  $d_{\text{diss}}$  on applied RF power for different  $\text{CH}_3\text{I}$  flows (in experiments  $\text{CH}_3\text{I}$  flows ranged from 0.1 to 0.77 mmol/s). Highest values of  $d_{\text{diss}}$  are near to 17% and with increasing donor flow the  $d_{\text{diss}}$  is decreasing. Iodine number density (concentration) increased with

number density was about  $2.5 \cdot 10^{14} \text{ cm}^{-3}$ , but further experiments need to be performed to see more complex dependencies. Up to now, the iodine concentration showed only a weak dependence on the donor flow rate, but it was rising with increasing RF power.

We can observe in both Figs. 4 and 5 that dissociation fraction depending on absorbed power is not saturated yet. That enables us to continue exploring higher discharge RF power and further experimental conditions until the saturation is achieved. Further, the role of reverse processes – back recombination of the dissociated donor, will be also investigated.

We started also using emission spectroscopy in later experiments, which proved the presence of excited iodine  $I(^2P_{1/2})$  in discharge and between 600 nm and 900 nm continuum spectrum was observed. This type of spectrum comes from recombination and bremsstrahlung.

## 5. Conclusion

New experimental device for generation of atomic iodine in RF discharge was built. This generator will be the part of DOIL (discharge oxygen-iodine laser) system. We performed first experiments with  $\text{CH}_3\text{I}$  and  $\text{CF}_3\text{I}$ , mainly for subsonic flows in the cavity. Experiments with these donors will continue and later new donors like  $\text{HI}$ ,  $\text{I}_2$ ,  $\text{C}_3\text{F}_7\text{I}$  will be also examined.

The donor with best operational characteristics will be selected and used for DOIL and also COIL operation.

In further experiments, we need to explore more characteristics in supersonic flow because, under such condition, supersonic cooling of the gas plays an important role and these conditions are very important for further lasing, higher temperature being detrimental to laser operation.

## Acknowledgement

This work has been supported by the European Office of Aerospace Research and Development (EOARD) under the Grant # FA8655-06-1-3034.

## References

- [1] P. V. Avizonis, G. Hasen, K. A. Truesdell: Proc. SPIE 1225 (1990) 448.
- [2] O. Špalek, M. Čenský, V. Jirásek, J. Kodymová, I. Jakubec, G. D. Hager: IEEE Journal of Quantum Electronics **40** (2004) 564.
- [3] J. Kodymová, O. Špalek, V. Jirásek, M. Čenský, G. D. Hager: Applied Physics A **77** (2003) 331.
- [4] T. Wakazono, K Hashimoto, T. Takemoto, T. Uchiyama, M. Muro: Proc. SPIE 3574 (1998) 290.
- [5] P. A. Mikheyev, A. A. Shepelenko, A. I. Voronov, N. V. Kupryayev: Journal of Physics D: Applied Physics **37** (2004) 3202.
- [6] A. P. Napartovich, A. A. Deryugin, I. V Kochetov: Journal of Physics D: Applied Physics **34** (2001) 1827.
- [7] J. Schmiedberger, V. Jirásek, J. Kodymová, K. Rohlena: Proceedings of 38th AIAA Plasmadynamics and Lasers Conference 4239 (2007).
- [8] U. Fantz: Plasma Sources Science and Technology **15** (2006) S137.
- [9] NIST International Database, [www.nist.gov](http://www.nist.gov).